

# Simple Modeling of Intrinsic Bulk Lifetime in Doped Silicon

Luigi Abenante<sup>a)</sup> and Massimo Izzi

*ENEA, Italian National Agency for New Technologies, Energy and Sustainable Economic Development, ROMA (Italy)*

<sup>a)</sup>Corresponding author: luigi.abenante@enea.it

**Abstract.** Based on the data in the literature, in highly-doped Si, where Auger recombination predominates, one can observe that, while minority-carrier bulk lifetime is inversely proportional to the square of doping density, diffusivity can be taken as constant. This implies that, at high dopings, diffusion length can be considered as proportional to the reciprocal of doping density. In the present work, we assume that such a dependence of diffusion length on doping holds at lower dopings as well, in the case, where Auger recombination prevails. This allows deriving a very simple expression for Auger lifetime as a function of diffusivity that is used together with a reported expression for radiative lifetime to calculate intrinsic lifetime at all dopings. The new expression for intrinsic lifetime is consistent with reported doping functions for minority-carrier diffusivity and agrees with the data of lifetime for dopings higher than  $4 \times 10^{17} \text{ cm}^{-3}$  in both *p*-type Si and *n*-type Si. We exploit the relevant theory to show that such results are due to the fact that, at those doping levels, both diffusivity and Auger recombination are enhanced by electron-hole interaction.

## INTRODUCTION

Lifetime measurements in highly doped Si and the Auger theory led Dziewior and Schmid to associate Auger recombination to a minority-carrier bulk lifetime proportional to  $N^{-2}$ , where  $N$  is the doping density [1]. We denote the Dziewior and Schmid  $N^{-2}$ -dependent Auger lifetime as  $\tau_{DS}$ . Afterwards, Yablonovitch and Gmitter detected  $N^{-2}$ -dependence of lifetime in lowly-injected Si wafers. To fit their data, however, they assigned to Auger lifetime,  $\tau_A$ , a dependence on  $N^{-1.65}$  [2]. Such proportionality to  $N^{-1.65}$  was retained by successive authors in both *n*- and *p*-type Si [3]. Recently, Richter et al. found that proportionalities to  $N^{-1.71}$  in *n*-type Si and  $N^{-1.73}$  in *p*-type Si are more correct, at least for  $N > 6 \times 10^{16} \text{ cm}^{-3}$  [4].

As a result,  $\tau_{DS}$  cannot characterize Auger recombination at all dopings. All of the authors in [2-4] admit nevertheless that, at high dopings, assuming  $\tau_A = \tau_{DS}$  is correct.

On the other hand, in the doping range, where  $\tau_A = \tau_{DS}$ , that is  $10^{20} > N > 10^{19} \text{ cm}^{-3}$ , it is commonly observed that diffusivity,  $D$ , varies very slowly with  $N$  (see Fig. 1). When  $\tau_A = \tau_{DS}$ , therefore,  $D$  can be assigned a constant value,  $D_A$  (see Fig. 1). Consequently, an Auger diffusion length,  $L_A$ , depending on  $N^{-1}$  is implied in the doping range, where  $\tau_A$  can be assigned  $\tau_{DS}$  and  $D$  can be assigned  $D_A$ .

In doping ranges, where  $\tau_A < \tau_{DS}$ , one can observe instead that  $D$  is higher than  $D_A$  and may vary rather quickly with  $N$ . In the present work, we assume that, in the case where Auger recombination prevails also at  $N < 10^{19} \text{ cm}^{-3}$ , assigning  $L_A = L_A(N^{-1})$  holds even if  $\tau_A < \tau_{DS}$  and  $D > D_A$ . Such an assumption implies that, rather than by lifetime, Auger recombination can be characterized by a diffusion length proportional to  $N^{-1}$ . It also implies a new very simple new expression for  $\tau_A$  as a function of  $D$  and  $D_A$ .

We exploit such a new function for  $\tau_A$  along with a reported function for radiative lifetime [4] in the expression for intrinsic lifetime,  $\tau_{intr}$ , of Richter et al. [eq. (15),4]. Fit functions to  $D$ -data available in the literature are implemented in the new  $\tau_{intr}$ -expression and  $\tau_{intr}$ -curves are obtained, which are in good agreement with lifetime data for  $N > 2 \times 10^{17} \text{ cm}^{-3}$ . We discuss such a result by exploiting the relevant theory. We show that, for  $N > 4 \times 10^{17} \text{ cm}^{-3}$ , diffusivity data can be fitted by the diffusivity component due to electron-hole interaction alone. On the other hand, according to the literature, at those doping levels, Auger lifetime is ruled by electron-hole interaction. As a result,

the reverse proportionality on  $N$  of diffusion length, which seems to be typical of Auger recombination, is preserved at  $N < 10^{19} \text{ cm}^{-3}$  as well.

## DERIVATION

In the high-doping range ( $N > 10^{19} \text{ cm}^{-3}$ ) after Dziewior and Schmid [1], Auger lifetime is given by [1–4]

$$\tau_{DS} = 1 / C_{DS} N^2 \quad (1)$$

where  $C_{DS}$  is the Dziewior and Schmid Auger coefficient relevant to the doping type [1].

In the same doping range,  $D$  can be assigned a constant diffusivity,  $D_A$  (see Figs.1 and 2). Hence, at high doping levels, an Auger diffusion length,  $L_A$ , can be assigned such that

$$L_A = \frac{1}{N} \sqrt{\frac{D_A}{C_{DS}}} \quad (2)$$

If we assume that (2) holds also at lower  $N$ -values, for which  $D > D_A$ , then an Auger lifetime,  $\tau_A$ , exists such that

$$\sqrt{D\tau_A} = \frac{1}{N} \sqrt{\frac{D_A}{C_{DS}}} \quad (3)$$

From (1)–(3), it follows that

$$\tau_A = \tau_{DS} \frac{D_A}{D} \quad (4)$$

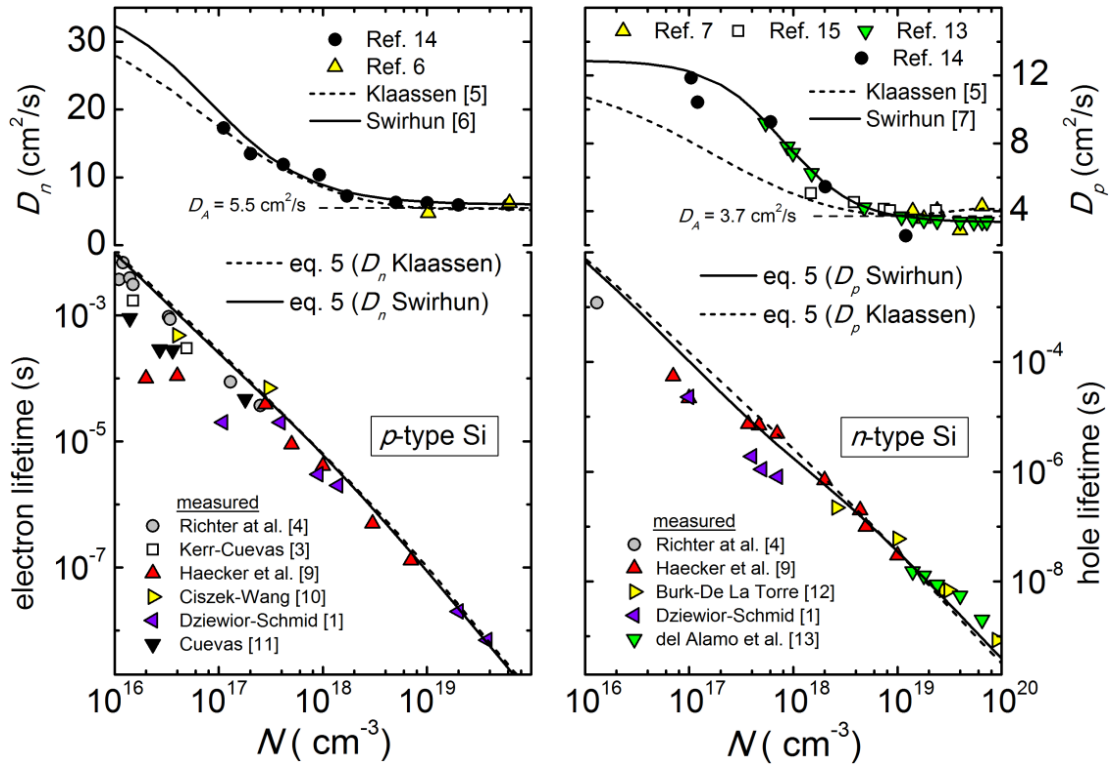


**FIGURE 1.** Curves of  $\tau_{intr}$  calculated with (5) (lines) are shown together with measured data of minority-carrier lifetime (symbols). In the upper panels, the  $D$  functions (lines) and  $D_A$ -values used to calculate with (5) the shown curves of  $\tau_{intr}$  are reported together with measured diffusivity values (symbols).

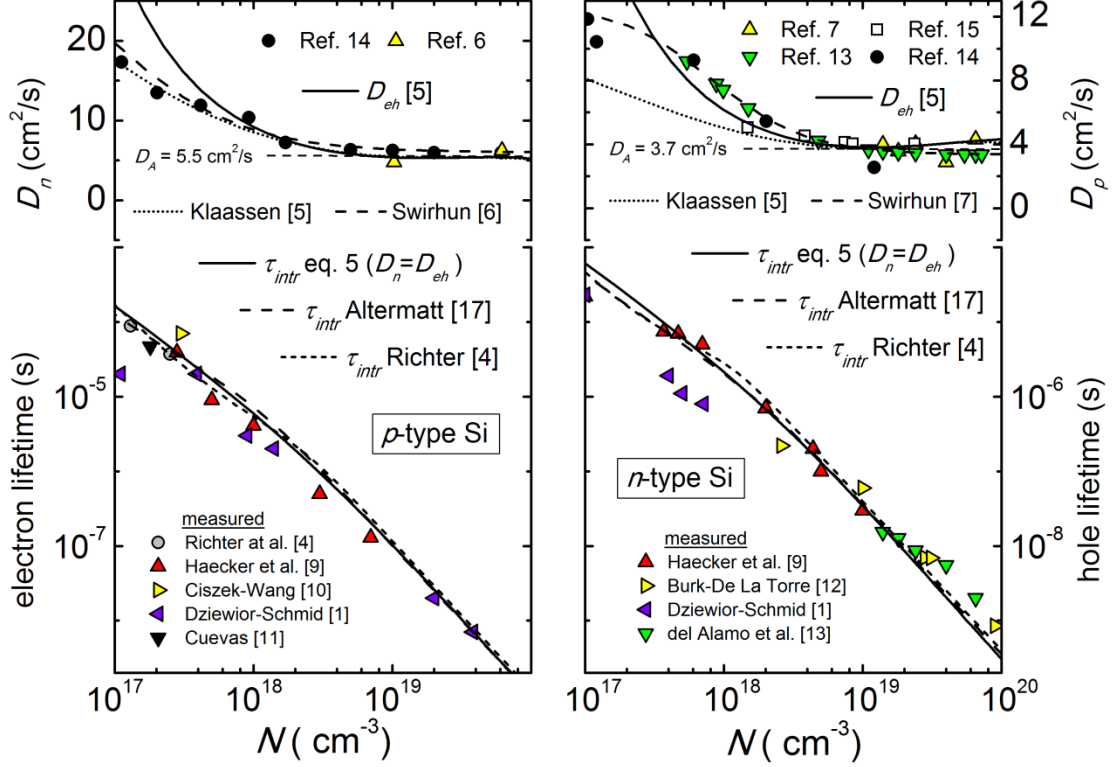


**FIGURE 2.** In the upper panels,  $D_{eh}$ -functions calculated after [5] (full lines) are reported together with measured diffusivity data (symbols) and the  $D$  functions used to calculate the  $\tau_{intr}$ -curves in Fig. 1. In the lower panels, the curves of  $\tau_{intr}$  relevant to the  $D_{eh}$ -functions are plotted as calculated with (5) at the shown  $D_A$ -values (full lines). Curves of  $\tau_{DS}$  (short-dotted lines) and measured data of minority-carrier lifetime (symbols) are also shown.

## APPLICATION

Eq. (4) was used, together with the expression for radiative recombination,  $\tau_{RAD}$ , from [4] to calculate the intrinsic lifetime,  $\tau_{intr}$ , after [4] as

$$\frac{1}{\tau_{intr}} = \frac{1}{\tau_A} + \frac{1}{\tau_{RAD}} \quad (5)$$

To this aim, available functions for  $D$  were implemented in (4). In Fig. 1, the  $\tau_{intr}(N)$ -curves are reported (lines), which were obtained with the shown  $D_A$ -values and  $D$ -curves taken from [5] and [6] for  $p$ -type Si and [5] and [7] for  $n$ -type Si. The curves of Klaassen [5] were calculated by the numerical program PC1D6 [8]. Measured data of minority-carrier lifetime and diffusivity are also plotted (symbols). As can be seen, both of the curves calculated with (5) can be considered as accurate for  $N > 4 \times 10^{17} \text{ cm}^{-3}$ .

## DISCUSSION AND CONCLUSION

In this section, we check the consistency of (4) with the modelling approach to Auger lifetime that takes into account an enhancement  $g$  of Auger recombination due to carrier interactions [4][16-17]. According to this model, at dopings lower than the Mott-transition concentration, Coulomb correlation predominates. At dopings higher than the Mott-transition concentration, instead, carrier-scattering processes predominate. Among such scattering processes, the electron-hole scattering is the most important [16-17].

In the model of Klassen for minority-carrier mobility [5], the contribution to diffusivity from electron-hole scattering,  $D_{eh}$ , can be calculated as a modification of the diffusivity due to donor scattering in  $n$ -type Si and acceptor scattering in  $p$ -type Si.

We have calculated  $D_{eh}$  at 300 °K in both  $p$ - and  $n$ -type Si. In Fig. 2,  $D_{eh}(N)$ -curves are compared to measured  $D$ -data and the curves for diffusivity at 300 °K used to obtain the  $\tau_{intr}$ -curves in Fig. 1. It is worth remarking that both the Klaassen curves for total diffusivity and  $D_{eh}$  are calculated by taking into account ultra-high doping ( $N > 10^{20} \text{ cm}^{-3}$ ) effects [5]. If these effects are neglected, then the humps at  $N > 10^{19} \text{ cm}^{-3}$  disappear and curves are nearly flat. Ultra-high doping effects have only been observed for majority-carrier mobility [5]. As can be seen,  $D_{eh}(N)$ -curves fit the diffusivity data for  $N > 4 \times 10^{17} \text{ cm}^{-3}$  in both  $p$ - and  $n$ -type Si and agree with the previously found  $D_A$ -values.

Eq. (4) was calculated at  $D = D_{eh}$  and inserted into (5) for both  $p$ - and  $n$ -type Si. The resulting  $\tau_{intr}(N)$ -curves are shown with full lines in Fig. 2, where they are compared to measurements and  $\tau_{intr}(N)$ -curves including  $g$  (dashed lines), which were calculated according the well-known models of Altermatt et al. [17] and Richter et al. [4]. As can be seen, the simple modeling approach to Auger lifetime presented in this work is consistent with Auger recombination enhancement due to carrier correlation for  $N > 4 \times 10^{17} \text{ cm}^{-3}$ . As can be seen in Fig. 2, within this doping range, the  $D$ -functions of Swirhun et al. [6-7] can be used instead of  $D_{eh}$ , which is more difficult to calculate. As a last remark, it is worth mentioning that (4), as well as (2), allows solving the minority-carrier transport equations in non-uniformly doped Si.

## REFERENCES

1. J. Dziewior and J. Schmid, *Appl. Phys. Lett.* 31, 346–348 (1977).
2. E. Yablonovitch and T. Gmitter, *Appl. Phys. Lett.* 49, 587 (1986); doi: 10.1063/1.97049
3. M. J. Kerr and A. Cuevas, *J. Appl. Phys.* 91, 2473–2480 (2002).
4. A. Richter, S. W. Glunz, F. Werner, J. Schmidt, and A. Cuevas, *Phys. Rev. B* 86, 165202 (2012).
5. D. B. M. Klaassen, *Solid-State Electron.* 35, 953–959 (1992).
6. S. E. Swirhun, Y. H. Kwark, and R. M. Swanson, *Int. Electron Devices Meet.* 32, 24–27 (1986)
7. S. E. Swirhun, J. del Alamo, and R. M. Swanson, *IEEE Electron Device Lett.*, EDL-7, 168–171 (1986).
8. H. Haug, A. Kimmerle, J. Greulich, A. Wolf, and E. Stensrud Marstein, *Sol. Energy Mater. Sol. Cells* 131, 30–36 (2014).
9. R. Haecker and A. Hangleiter, *J. Appl. Phys.* 75, 7570 (1994)
10. T. F. Ciszek and T. H. Wang, in *Proceedings of the 14th European Photovoltaic Solar Energy Conference* (1997) p. 103.
11. A. Cuevas, *Sol. Energy Mater. Sol. Cells* 57, 277–290 (1999)
12. D. E. Burk and V. de la Torre, *IEEE Electron Device Lett.* EDL-5, 231–233 (1984)
13. J. A. del Alamo and R. M. Swanson, *IEEE Trans. Electron Device* 34, 1580–1589 (1987)
14. J. Dziewior and D. Silber, *Appl. Phys. Lett.* 35, 170–172 (1979)
15. Chih Hsin Wang, K. Misiakos, and A. Neugroschel, *IEEE Trans. Electron Device* 37, 1314–1322 (1990)
16. A. Hangleiter and R. Haecker, *Phys. Rev. Lett.* 65, 215 (1990).
17. P. P. Altermatt, J. Schmidt, G. Heiser, and A. G. Aberle, *J. Appl. Phys.* 82, 4938 (1997)